IEEE Robotics and Automation Letters (RAL) paper presented at the
2020 IEEE/RSJ International Conference on Intelligent Robots and Systems (IROS)
October 25-29, 2020, Las Vegas, NV, USA (Virtual)

A Dexterous Soft Robotic Hand for Delicate In-Hand Manipulation

Sylvain Abondance*[1,2], Clark B. Teeple*[1], and Robert J. Wood[1]

***Abstract*— In this work, we show that soft robotic hands provide a robust means of performing basic primitives of in-hand manipulation in the presence of uncertainty. We first discuss the design of a prototype hand with dexterous soft fingers capable of moving objects within the hand using several basic motion primitives. We then empirically validate the ability of the hand to perform the desired object motion primitives while still maintaining strong grasping capabilities. Based on these primitives, we examine a simple, heuristic finger gait which enables continuous object rotation for a wide variety of object shapes and sizes. Finally, we demonstrate the utility of our dexterous soft robotic hand in three real-world cases: unscrewing the cap of a jar, orienting food items for packaging, and gravity compensation during grasping. Overall, we show that even for complex tasks such as in-hand manipulation, soft robots can perform robustly without the need for local sensing or complex control.**

I. Introduction

Manipulating objects in the real world usually requires robots to accommodate a relatively large degree of uncertainty in the shape, size, and pose of objects in the environment [1]. In addition to environmental uncertainty, target objects are often located in highly-constrained positions, or must be placed into new positions that are outside the dexterous workspace of the arm. Target objects or world features are also commonly fragile or delicate, especially in applications within the home. Many activities of daily life (ADL) involve all three of these challenges [2], such as setting a table with fragile dishes or storing delicate produce items in a refrigerator without bruising them.

Another useful skill for real-world manipulation is the ability to change an object's pose without using external surfaces, even when the arm's range of motion is limited in some way. For example, re-grasping an object to improve the grasp quality has been studied extensively [3], [4]. However, most examples require the robot to set down the target object on a tabletop before re-grasping. This workflow relies on reasonably accurate models of the object's dynamics, environment geometry, and contact dynamics in addition to the robot's own dynamics [5], [6]. Alternatively, if robots can manipulate the object within their hands, grasps can be adjusted without relying on external surfaces.

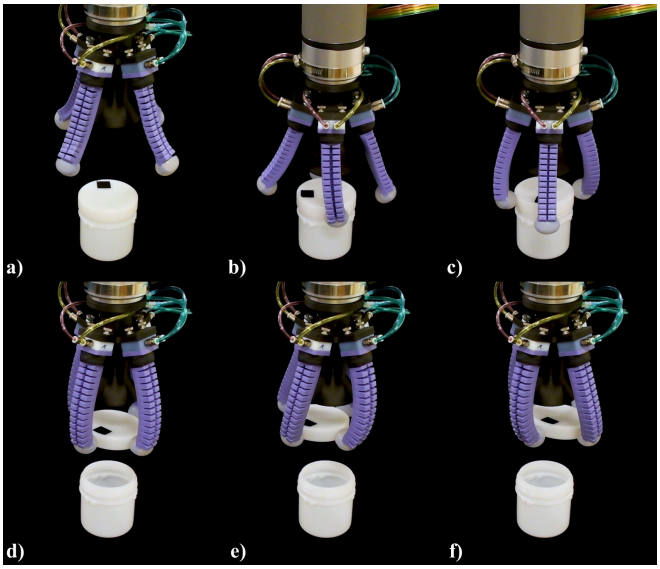

Fig. 1. Our soft, dexterous hand prototype is capable of performing real-world manipulation tasks within the hand. a)-c) The hand is shown unscrewing the cap of an empty plastic jar using a heuristic finger gait for rotation. d)-f) The hand can also impart planar translations to objects. The empty jar was lightly taped to the ground to enable un-capping.

In recent years, there has been a sizable push toward utilizing compliant robotic hands that passively adapt to uncertainty in the environment [7]. Soft-bodied hands enable robots to grasp objects of varying shape, size, and pose without explicit knowledge of those properties [8], [9], [10], [11]. Furthermore, passive compliance enables robots to safely interact with delicate target objects or other fragile features in the environment [12], [13], [14].

Dexterous in-hand manipulation usually requires precise planning and control of finger motion based on models of the object and fingers when performed by rigid hands [15], [16], [17]. This is due to complex contact interactions between the fingers and object, as well as minimal passive adaptation to object variation. Some attempts to mitigate the complexity of these interactions using machine learning show incredible promise, but require extensive training on high performance computing systems [18]. However, we can mitigate the need for planning and complex control for some in-hand manipulation tasks through targeted design of a soft robotic hand with dexterous fingers.

In this paper, we show that soft robotic hands can robustly perform in-hand manipulation in the presence of uncertainty. We first design a soft hand prototype with dexterous fingers capable of fingertip motion conducive to several basic motion primitives. Through empirical validation, we show that these

* The first two authors contributed equally to this work.

[1]John A. Paulson School of Engineering and Applied Sciences, Harvard University, 60 Oxford St. Cambridge MA 02138, USA

[2]École polytechnique fédérale de Lausanne (EPFL), Route Cantonale, 1015 Lausanne, Switzerland

All correspondences should be addressed to Clark Teeple or Robert Wood (cbteeple@g.harvard.edu, rjwood@seas.harvard.edu).

This work was supported by the Wyss Institute for Biologically-Inspired Engineering and the National Science Foundation (award #EFMA-1830901).

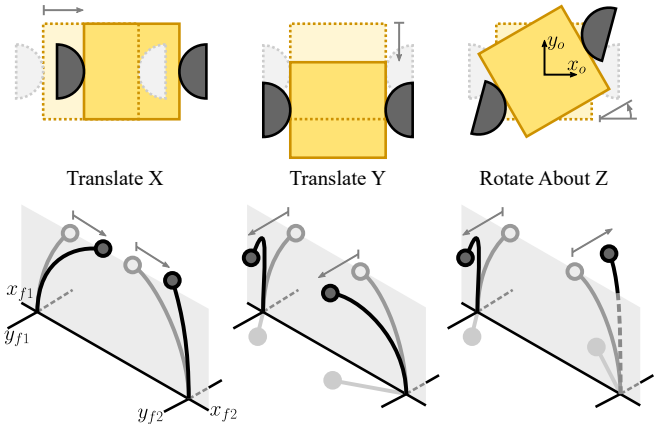

Fig. 2. The necessary fingertip motions for our soft hand are conceptually derived from desired object motion primitives. Based on the motion of typical soft bending actuators, the desired fingertip motions can be achieved using two parallel bending actuators

dexterous fingers enable the desired object motion primitives within the hand while still maintaining strong grasping capabilities. We then examine a simple, heuristic finger gait which enables continuous object rotation for a wide variety of object shapes and sizes. Finally, we demonstrate the utility of in-hand manipulation using a dexterous soft hand in three real-world cases: unscrewing the cap of a jar, orienting food items for packaging, and gravity compensation during grasping.

II. Design of a Dexterous Soft Hand

A. Task-Centric Performance Goals

In this work, we focus on three motion primitives in which the object moves while maintaining a grasp: rotation about one axis, and translation in two axes of a plane, as displayed in Figure 2. These primitives were chosen based on their utility in a set of target tasks drawn from a variety of application areas. These areas include performing ADL in the home, assembling and packaging delicate items such as pastries [19], and picking/handling produce [20].

Our first desired motion primitive is rotation about an object's central axis. Rotation is useful for a variety of activities of daily life including unscrewing bottle caps, turning dials and knobs, and reorienting non-axisymmetric objects. Rotations can also enable tool use during assembly, adjustment of items during packing tasks, and twisting fruits and vegetables to pick them.

The second and third target motion primitives are translations in the plane perpendicular to the object's central axis. Planar translations are useful for fine, local adjustments during packing tasks, as well as picking produce by shifting side-to-side. Furthermore, translations can be used to compensate for finger deflection caused by gravitational forces on the object.

B. High-Level Hand Design

To build a soft hand capable of achieving the three motion primitives of interest, several design decisions were made based on previous successful hand designs with compliant

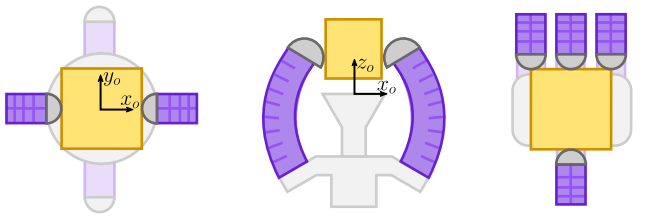

a) Four-Finger Cross **b)** Anthropomorphic

Fig. 3. The two high-level hand designs considered in this work are the a) four-finger cross design, and b) more-traditional anthropomorphic design.

fingers. The high-level structure of the hand was designed with several compliant digits placed around a flat palm. The axis normal to the palm was set to be parallel to the object's central axis so the rotations and translations occur in the reference frame attached to the palm. To simplify object motions, the fingers and palm were designed such that objects only contact fingers at the fingertips. We also assume fingertips have rolling contact with objects without slipping.

Additionally, two high-level configurations were considered for finger arrangement: four-finger cross, and anthropomorphic, as displayed in Figure 3. The four-finger cross configuration has two sets of antipodal finger pairs, similar to several existing hands [21], [22]. Conversely, anthropomorphic configuration is based on the designs of several soft hands [9], [10], [11].

Considering these two hand configurations, we ultimately chose the 4-finger cross design, as it appears to simplify the control of our three target motion primitives. Under open-loop pressure control, this hand design makes it easier to control translation compared to the anthropomorphic hand, where more than two fingers are implicated for the same translation. Finally, many common objects in the home have aspect ratios of $\sim$1:1:1 [23], making the four-finger cross the best choice due to symmetry between pairs of fingers. An in-depth discussion of the manipulation capabilities of these two hand designs can be found in the Supplementary Materials.

C. Dexterous Finger Design

In order to design dexterous soft-bodied fingers, we used an object-centric approach to extract how the fingertips should move based on our desired object motion primitives, as shown in Figure 2. To produce object translations, fingertips need to translate in the primary grasping axis (in/out toward the center of the palm) and side-to-side (perpendicular to the grasping axis). Side-to-side motion is also necessary to perform rotatory motion of the grasped object. In addition to fingertip motion, the fingers must be strong enough to impart that motion onto real objects as well as sustain strong grasps along the grasping axis.

To achieve compliant, strong, and lightweight fingers, we created pneumatic bending actuators with two side-by-side air chambers separated with a central wall. Each chamber is based on a typical bellows actuator design, similar to those found in [12]. This configuration of actuators enables

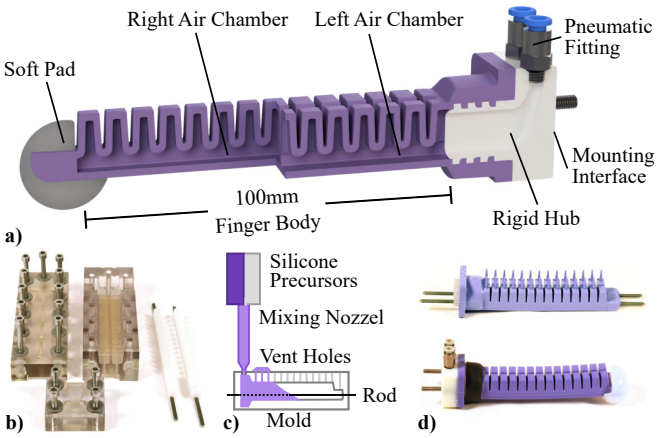

Fig. 4. The design and fabrication of our two-chamber dexterous fingers. a) Our finger design utilizes two side-by-side bellows actuators. b)-d) The fabrication process for these fingers involves injecting silicone elastomer into 3D-printed molds with soft cores.

strong grasping when both chambers are actuated with equal pressure, while also offering ample side-to-side motion when actuated differentially. In addition, the side-to-side motion can be amplified by using vacuum to increase the pressure differential between chambers. A more-detailed explanation of how actuation pressures affect fingertip motion can be found in the Supplementary Materials.

We carried out several design iterations in an attempt to maximize the strength, range of motion, and burst pressure of these fingers to increase the reliability of this system. Several design parameters were modified including the number and size of bellows, wall thickness, and fingertip shape. The most recent version presented in Figure 4a has 14 short bellows with a wall thickness of 2mm. We chose a bending segment of 100mm and a width of 22.5m to maintain consistency with similar designs such as [24], [12]. Soft finger pads were added to each fingertip to increase compliance with grasped objects [25], [26].

D. Hardware Fabrication

The fabrication process for our soft fingers is based on the process found in [12], a rigid mold creates the outer geometry of the finger, and a soft silicone core creates the internal geometry. Before building a finger, two soft cores are made by injecting True Skin®10 silicone into a 3D printed mold (VeroClear, Stratasys), then curing in an oven for one hour. To build a finger, the two soft cores are de-molded and secured in the main mold using two square rods, as shown in Figure 4b. Next, all parts of the mold are clamped together with screws, and Smooth-Sil™945 silicone (45 Shore-A hardness) is injected using a custom injection system, as shown in 4c. When the material is cured, the two soft cores are removed, resulting in the two side-by-side air chambers. The two holes created by the rod are sealed with a small amount of silicone to prevent air leakage. The soft finger pads are created using the same injection process but with a softer silicone (Ecoflex 00-30™) with a 30 Shore-00 hardness. The injection process ensures that the fingers are made repeatably, with minimal variation between each batch.

To complete a newly molded finger, first a 3D printed hub with ribs is fitted with two pneumatic fittings enabling easy swapping of pneumatic control lines, and two screw posts for mounting on the scaffold. This hub is then glued into the main body of the finger with Sil-Poxy™. A Kevlar thread binding and heat shrinking tubing is fixed around the base of the finger to strengthen the pneumatic connection between the rigid hub and the finger body. The completed finger can be seen in Figure 4d. All of the molds and the rigid hubs were 3D printed on an Object Connex 500 printer (VeroClear, VeroWhite and VeroBlue, Stratasys).

Once four fingers are completed, they are attached to a rigid scaffold to arrange them into two perpendicular antipodal finger pairs. The finger mounting angle was chosen based on the fingers' range of motion. An angle of 40° between the two fingers in each pair permits grasping a wide variety of objects without losing force before making contact with the object. Since the scaffold has the same mechanical interface as the fingers and palm, it is easy to swap new fingers and palms as needed. The scaffold is also designed to be easily attached to a robotic arm (UR5e) with a standard mounting flange.

Finally, a palm is placed in the middle of the scaffold, with a flat surface of 70 mm diameter located at a distance of 40 mm from the contact point of the fingertip. This palm height ensures that objects are close enough to the fingertips when resting on the palm. Both the scaffold and rigid palm were 3D printed on a Markforged Onyx One printer (Onyx Material, Markforged).

III. Characterization of the Hand Prototype

A. Actuation and Control

To control pressures independently on both sides of each finger, we used a custom pneumatic pressure control system with eight independent channels [27]. Based on the system used in [24], the controller enables execution of arbitrary pressure trajectories in real time with an accuracy of 1.4 kPa. Detailed performance specifications can be found in the Supplementary Materials.

B. Finger Performance

Before characterizing the hand, we first characterized fingers individually to understand the range of motion, strength, and operating pressures. These metrics subsequently inform how fingers can be used for grasping and manipulation within the hand.

To evaluate the workspace of our soft, 2DOF fingers, we applied sweeps of actuation pressure/vacuum to both chambers of the finger(-34 kPa to 240 kPa), and measured the free deflection of the fingertip. Using a Vicon motion capture arena, a finger's workspace was traced out in 3D, and the resulting surface is shown in Figure 5a. The fingertips have a range of approximately 80 mm in the major grasping axis, and $\pm$ 30 mm of lateral range with minimal change in grasping displacement.

In addition to the 3D workspace, the grasping axis curvature in response to actuation pressure can help us understand

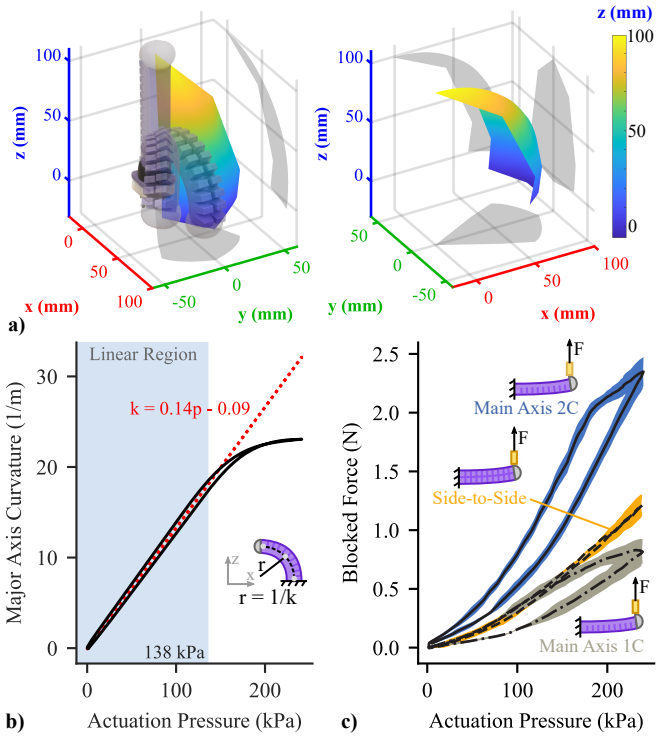

Fig. 5. Validation of finger performance. a) The workspace of our fingers enables ample side-to-side motion during a grasp. Two views of the fingertip workspace surface are shown. b) The curvature in the grasping axis vs. actuation pressure is roughly linear in the 0 kPa to 138 kPa range. c) The maximum blocked force of each finger is 2.3 N in the grasping axis, and 1.2 N side-to-side.

how to control these fingers. To measure the curvature of fingers along the main grasping axis, we applied controlled pressures equally to both actuator chambers, and measured the resulting displacement of three points along the length of a finger. Using MATLAB to synchronize the motion tracking data to actuation pressure, we pressurized the finger from 0 kPa to 250 kPa. Then, the curvature was computed from the marker positions using a least squares fit for a circle. The results are shown in Figure 5b. The curvature linearly increases with pressure from 0 kPa to 138 kPa, after which minimal change in curvature occurs. This suggests an operating point of 138 kPa during grasping is a reasonable starting point.

To evaluate the strength of our soft fingers, we began by measuring the blocked force during actuation. Individual fingers were placed in a custom fixture beneath the crosshead of an Instron universal testing machine with a 10N load cell. The fingers were actuated from 0 kPa to 250 kPa, and the resulting vertical blocked force was measured, as shown in Figure 5c. Each test was repeated three times for three different fingers. The maximum strength in the grasping axis is 2.3 N when both air chambers are pressurized. However, the strength when only one air chamber is pressurized is 0.8 N in the grasping axis and 1.2 N side-to-side, indicating a tradeoff in grasping forces vs. side-to-side motion.

Another useful performance metric is the unactuated stiffness, which can help us understand finger behavior under load. To measure the stiffness, we used a custom fixture to mount fingers as cantilevers underneath the crosshead of the Instron. We then used the Instron to deflect the finger by 10 mm along the x and y axes of the finger while measuring the resulting force. We then found the slope of the load-displacement curve for each sample, which results in the average stiffness shown in Table I. It is notable that our finger design is approximately 4.7 times stiffer in the side-to-side axis than the grasping axis, which can potentially help maintain stable grasps when fingertip forces are not perpendicular to the grasping axis.

TABLE I

UNACTUATED STIFFNESS OF INDIVIDUAL FINGERS IN EACH AXIS.

	Unactuated Stiffness (N/m)	
	Grasping Axis	**Side-to-Side**
Finger 1	6.09 ± 0.03	28.23 ± 0.20
Finger 2	6.23 ± 0.07	28.90 ± 0.11
Finger 3	6.04 ± 0.02	30.02 ± 0.16
Total	6.12 ± 0.09	29.05 ± 0.8

* The mean and standard deviation are reported for $n = 3$ trials for each sample.

Finally, we obtained a burst pressure of 310 kPa for both air chambers. Actuation pressure was slowly increased at approximately 10 kPa per second until the fingers failed by rupturing. Combined with the results of our curvature evaluation, we chose 240 kPa as the maximum operating pressure and 138 kPa as the nominal grasping pressure.

C. Grasping Performance

With a better understanding of the performance of individual fingers, we now focus on the grasping performance of the whole four-fingered hand. Through an analysis of the grip strength and grasp stiffness, we determined the range of object masses that can be sustained in a grasp, as well as how hand orientation affects this.

To measure the grip strength of our soft hand as well as the effect of soft finger pads on grasping performance, we performed a series of grasps on a cylinder of diameter 76.2mm similar to [12]. The cylinder was attached to the crosshead of our Instron machine, and the hand was fixed on a structure below the cylinder. The cylinder was then pulled vertically and the maximum vertical force from the fingers was measured. This process was repeated three times for each hand configuration. With this setup, we evaluated the effect of the actuation pressure, soft finger pads, and the use of two vs. four-fingers on grasp strength, as displayed in Figure 6a.

Based on our experiments, the hand has the highest grip strength when using four fingers with soft finger pads actuated at the highest pressure. With a pressure of 173 kPa, the hand achieves a grip strength of 4.7N, demonstrating that the hand is able to grasp objects up to 0.47kg when four fingers are actuated with soft finger pads. Conversely, the best possible performance without finger pads was only 0.21N (grasping a 0.21kg object), showing that adding soft pads significantly increases grip strength. Finally, our experiments

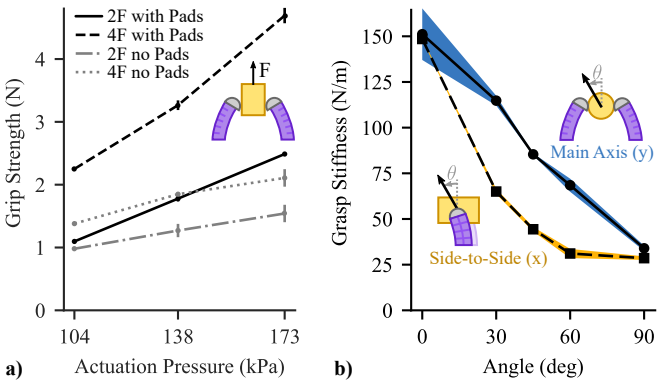

Fig. 6. Characterization of grasping performance. a) The grip strength increases by a factor of two when compliant finger pads are used compared to harder fingertips. b) The grasp stiffness decreases roughly linearly with the angle along the main axis, but much faster side-to-side. In both graphs, the mean and standard deviation are reported for $n = 3$ trials for each sample.

show that grip strength is roughly two times higher when grasping with four fingers compared to two fingers.

In addition to grasping strength, the hand must also be able to resist external forces applied off-axis. To evaluate the hand's ability to resist off-axis loading, we measured the stiffness of two-finger grasps as a function of the angle. For these measurements, a cylinder of 25 mm diameter was fixed to the crosshead of the Instron, and the hand was mounted at precise angles to the cylinder using a custom fixture. To measure stiffness, a two-finger antipodal grasp was performed on the cylinder (with an actuation pressure of 138 kPa), then the cylinder was deflected by 10 mm using the Instron and the resulting vertical force was measured. This process was repeated three times for angles ranging from 0 to 90 degrees about the x and y axes.

The resulting grasp stiffness for angles about both axes is presented in Figure 6b. For angles about the major axis of the cylinder (x-axis), the grasp stiffness decreases roughly linearly with angle, similar to the fingers in [24]. In addition, the stiffness decreases much quicker for angles about the y-axis (side-to-side with respect to the antipodal grasp). This discrepancy is likely due to the added stiffness of each finger in the grasping direction when actuated with air pressure. Finally, the worst-case loading condition involves forces perpendicular to the palm (90°) where the stiffness is lowest (30–35 $\mathrm{N\,m^{-1}}$). In practical use, this suggests a 50 g object held perpendicular to gravity would deflect by 17 mm.

IV. In-Hand Manipulation Primitives

To evaluate the in-hand manipulation performance of our prototype hand, we empirically tested all three motion primitives using a small standard set of objects, as shown in Figure 7a. To keep consistent with standard object sets, two rigid cylinders were taken from the YCB Object set (47 mm and 88 mm diameters), and a rigid box of dimensions 60 mm × 60 mm × 60 mm was included from [24]. In addition to these rigid objects, a compliant box made of memory foam (50 mm × 50 mm × 70 mm) was used. Finally, three fragile real-world objects were tested: two muffins (70 mm

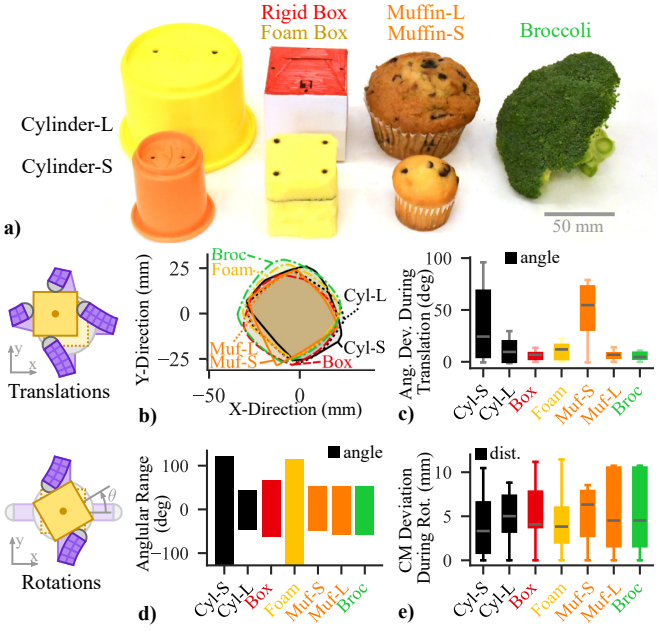

Fig. 7. a) Our soft hand can perform the three object motion primitives for which it was designed on a variety of objects. b) The space of reachable object translations is similar for all objects tested. c) The undesired angular motion of the object during one translation cycle is somewhat large. d) The range of reachable object rotations is highly dependent on object size. e) The extra translational motion of the object during one rotation cycle is within 12 mm for all objects.

and 40 mm diameters), and a broccoli crown (approximately 110 mm diameter). The masses and dimensions of all objects can be found in the Supplementary Materials.

To evaluate the spatial range of object motions our hand is capable of achieving, we performed sweeps over all three motion primitives. Using heuristically-designed pressure trajectories (sequences of hand-tuned pressure waypoints), finger motion was commanded slow enough to assume quasi-static conditions. The motion primitives were carried out with objects starting at rest on a transparent acrylic ground plane, and object motion was captured using a camera mounted below. Using Tracker Video Analysis software [28], we measured the positions of two known markers on each object, enabling the object's planar pose to be calculated using Python.

The planar "workspace" for each object is shown in Figure 7b and 7d. The region of reachable positions in the x-y plane is similar for all objects, with a roughly circular shape of 50 mm diameter. This region is likely limited by the size of each finger's workspace, with ±30 mm of side-to-side deflection. Conversely, the range of reachable object rotations is inversely dependent on object size, with smaller objects undergoing larger rotations. This also meets expectations given the range of side-to-side deflection each finger can achieve. Finally, while knowledge of object size could be used to calculate the necessary finger motion to achieve a given rotation angle, this relationship is highly nonlinear.

When commanding pure motion primitives on the object, we also measured the object's undesired off-axis motion, as shown in Figure 7c and 7e. During the sweep of reachable

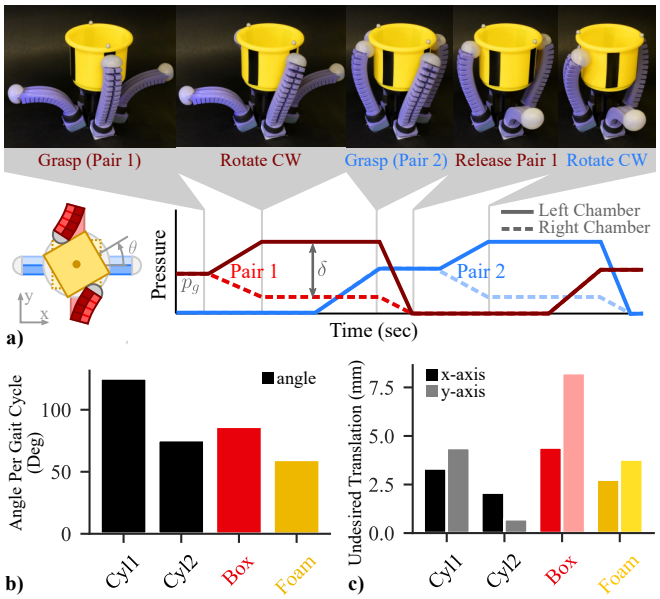

Fig. 8. Using a simple heuristic finger gait, our soft hand is capable of continuously rotating a variety of object shapes and sizes. a) The rotation gait is defined via actuation pressures, and photographs of key events in the gait are displayed. Unless noted, p_g = 138 kPa and δ = 34 kPa b) The angular displacement per gait cycle is reported for $n = 20$ cycles per object (mean and standard deviation). c) The undesired lateral object motion is similar in magnitude to that seen during the rotation primitive. † The palm was raised by 10 mm and δ = 28 kPa. †† The palm was raised by 10 mm and p_g = 172 kPa.

translations, smaller objects tended to incur larger undesired angular deflection. This is likely due to rotational instabilities that occur when grasping objects of smaller diameter (higher curvature) [26]. On the flip side, the uncontrolled lateral translation during attempts to achieve pure object rotation were small compared to object dimensions (within 12 mm for all objects).

The effect of irregularities in object shape can be derived from the results of individual objects. Pure translation appears to be relatively invariant to object size, so objects with protrusions or extreme aspect ratios could still be manipulated predictably. Conversely, pure rotation is very dependent on the distance between fingertips, so we expect that objects with lobes or extreme aspect ratios would experience rotation similar to simpler objects of the same diameter for any given set of contact points.

V. A Simple Finger Gait for Continuous Rotation

While simple combinations of our desired motion primitives enable considerable object motion, these primitives have limited spatial range if the finger maintains contact with the object. However, if contact with the object can be broken and reformed once the fingers reach the edge of their workspace, a finger gait can be developed to move objects an arbitrary amount. Our hand design with two pairs of antipodal grasping fingers can perform such finger gaits stably within the hand, and without placing the object onto an external surface during the reset period.

Focusing on continuous object rotation, we can utilize the compliance of our soft fingers to design one simple finger gait that enables continuous rotation of a wide variety of objects. The gait involves a two-part cycle with two parameters based on an extension of our simple rotation primitive, as shown in Figure 8. First, the object is grasped with one pair of antipodal fingers and rotated to the edge of the fingertip's workspace while maintaining contact. Next, the other two fingers form an antipodal grasp on the object while the first grasping pair holds position. From here, the first grasping pair releases while attempting to maintain the fingers' lateral positions, then the pair is reset to its resting position. Finally, the second part of the cycle is identical to the first part except the roles of the grasping pairs are flipped. The gait can be defined entirely in actuation pressure space, with a nominal grasping pressure, p_g, and a deviation from that pressure, δ, which differentially actuates the two fingers to produce rotation.

We evaluated the utility of this finger gait by testing its performance on our previously defined set of objects. The results of these tests are shown in Figure 8. For each object, we performed the finger gait for 20 gait cycles while capturing the resulting object motion using a Vicon motion capture system. The average number of cycles to rotate each object are shown in Figure 8, along with the average extraneous lateral motion.

Not only is this class of finger gaits simple, the gait is also robust to variation in object shape and size. In fact, for this set of experiments, the exact same actuation pressure trajectories were used for all objects, which still resulted in successful, continuous object rotation for all 20 gait cycles. We suspect the mechanism that this simple finger gait exploits is the fact that controlling actuation pressure indirectly controls contact forces on the object. Using pressure control on a soft finger results in controlling finger motion until the finger is blocked, then acts as contact force control on the object [29]. This means that we can achieve robust continuous object rotations without fingertip sensors, and without re-planning fingertip trajectories in response to object size and shape differences. Moreover, this continuous object rotation is useful when a robotic arm is constrained by the environment or reaches joint limits. This continuous motion can also be advantageous in arms that do not have rotational wrists.

VI. Demonstration of Real-World Manipulation

To showcase the utility of our soft dexterous hand, three manipulation tasks were performed using a UR5e 6-DOF robot arm. While visual perception is essential to any full manipulation system [1], no visual perception was used as it is outside the scope of this study. In these demonstrations, objects are manually placed, and the arm moves our dexterous hand to predefined poses without explicit knowledge of the object's pose, size, or mass properties (unless noted). Full motion sequences for all of these demonstrations can be found in the Supplementary Video.

In the first task, our soft hand is used to un-screw the cap of a plastic jar (as shown in Figure 1), a common activity of daily life. Using our simple finger gait for continuous

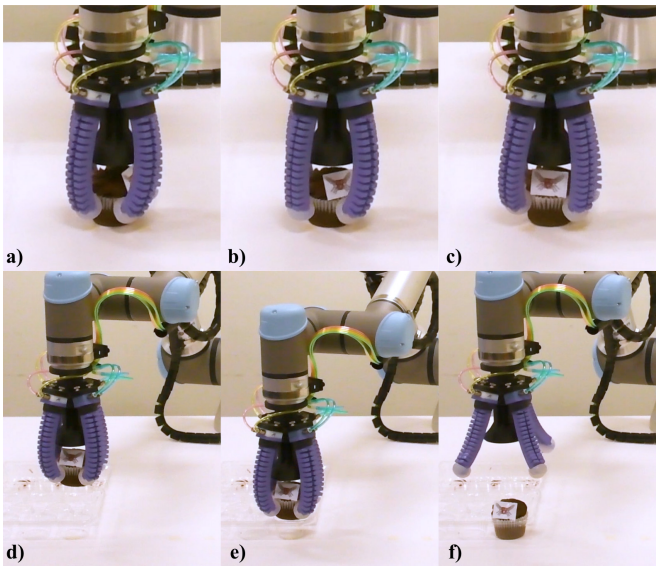

Fig. 9. Using the heuristic finger gait developed earlier, our soft hand can gently manipulate delicate objects. a)-b) The hand rotates a cupcake to place a design in a desired orientation (forward). c) The hand then grasps the cupcake. d)-f) Finally, cupcakes are packed in a carton with the help of a robot arm. The full sequence is shown in the Supplemental Video.

rotation, the cap is successfully removed and picked up by the arm. Then the x-y translation primitives are combined to move the cap in mid-air without the use of an external surface. The cap is then replaced, and the whole jar is grasped and translated in mid-air.

In addition to rigid objects, soft hands can gently manipulate delicate objects such as fruits, vegetables, or pastries [19]. For example, the task of packing cupcakes into a container is easily performed using our dexterous soft hand, as demonstrated in Figure 9. Furthermore, we can utilize our simple finger gait to rotate the cupcakes prior to packing, placing a design forward in the container.

Finally, the dexterity of the two-chamber fingers in our hand can be used to compensate for finger droop caused by the weight of grasped objects. Finger deflections during a grasp are usually large for soft robotic hands, including ours, relative to the mass of typical objects due to high finger compliance. Given knowledge of the hand's orientation and approximate object mass, a translation primitive (simple pressure offsets) can be applied to each section of the rotation gait to shift the fingertip position vertically and recover from finger droop, as shown in Figure 10.

Compensating for finger droop is often crucial to the success of the rotation task for our soft hand. As demonstrated in Figure 10, when the fingertips are not shifted to account for droop, the object is dropped during the rotation gait attempt. However, when the gait is gravity compensated, the object's position is closer to the center of the palm during the rotation, and stable rotation is achieved. Thus, designing fingers and a hand with the capability to translate objects enables soft hands to manipulate objects in a much wider variety of orientations.

VII. Conclusions and Future Work

In summary, we demonstrated that a soft robotic hand is capable of robust in-hand manipulation of delicate objects without knowledge of the precise position, shape, or size of those objects. Through a conceptual analysis of desired object motion, we designed a soft hand with four soft, dexterous fingers capable of moving objects in a plane. Using simple control, our soft hand can achieve three object motion primitives (translation and rotation in a plane), which can be combined in a straightforward way. In addition, using a simple heuristic finger gait, the hand can achieve continuous rotation of objects. Finally, we demonstrated three real-world tasks where our dexterous soft hand utilizes in-hand manipulation to maneuver objects in a gentle way.

In future work, there is endless potential to dive deeper into soft manipulation. We expect that a palm made of soft components will enhance the performance of in-hand manipulation. Manipulation of grasped objects could be further improved using mathematical models of finger motion, and on-board sensing of finger shape or contact forces. With these tools, closed-loop control of contact forces could provide even more-robust manipulation in cases where passive compliance fails. Finally, dexterous soft robotic hands could be applied to a variety of exciting applications, from in-home assistive robots to bimanual manipulation, since soft robotic hands can interact safely with themselves and the surrounding environment.

Acknowledgements

The authors thank Michael Bell and Luca Cattani for their essential discussions on fabrication of soft actuators. The authors also thank Kaitlyn Becker for her expertise in and discussions on soft actuator design. Furthermore, we thank Moritz Graule, Ted Sirota, and James Weaver for their helpful discussions throughout the design process.

This work was supported by the Wyss Institute for Biologically Inspired Engineering; the National Science Foundation (award number EFMA-1830901); and the National Science Foundation Graduate Research Fellowship (under grant DGE1745303). Any opinions, findings, conclusions, or recommendations expressed in this material are those of the authors and do not necessarily reflect those of the funding organizations.

References

[1] M. T. Mason, "Toward robotic manipulation," *Annual Review of Control, Robotics, and Autonomous Systems*, vol. 1, pp. 1–28, 2018.

[2] I. M. Bullock, R. R. Ma, and A. M. Dollar, "A hand-centric classification of human and robot dexterous manipulation," *IEEE Transactions on Haptics*, vol. 6, no. 2, p. 129–144, Apr 2013.

[3] A. Fernandez, J. P. Gazeau, S. Zeghloul, and S. Lahouar, "Regrasping objects during manipulation tasks by combining genetic algorithms and finger gaiting," *Meccanica*, vol. 47, no. 4, p. 939–950, Apr 2012.

[4] A. Bicchi, "Hands for dexterous manipulation and robust grasping: a difficult road toward simplicity," *IEEE Transactions on Robotics and Automation*, vol. 16, no. 6, p. 652–662, Dec 2000.

[5] N. C. Dafle, A. Rodriguez, R. Paolini, B. Tang, S. S. Srinivasa, M. Erdmann, M. T. Mason, I. Lundberg, H. Staab, and T. Fuhlbrigge, "Extrinsic dexterity: In-hand manipulation with external forces." IEEE, May 2014, p. 1578–1585.

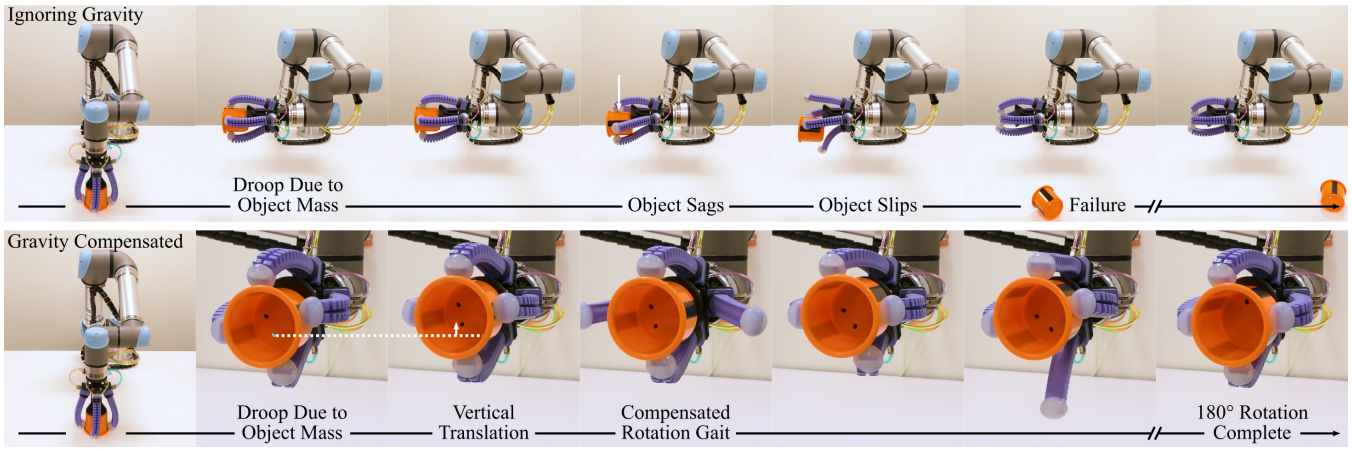

Fig. 10. By combining motion primitives (translation + rotation), the hand can adjust the object's position to compensate for finger droop caused by gravity. The full, annotated motion sequence can be found in the Supplementary Video.

[6] N. Furukawa, A. Namiki, S. Taku, and M. Ishikawa, "Dynamic regrasping using a high-speed multifingered hand and a high-speed vision system," in *2006 IEEE International Conference on Robotics and Automation, 2006. ICRA 2006.* IEEE, 2006, p. 181–187.

[7] D. Rus and M. T. Tolley, "Design, fabrication and control of soft robots," *Nature*, vol. 521, no. 7553, p. 467, 2015.

[8] L. U. Odhner, L. P. Jentoft, M. R. Claffee, N. Corson, Y. Tenzer, R. R. Ma, M. Buehler, R. Kohout, R. D. Howe, and A. M. Dollar, "A compliant, underactuated hand for robust manipulation," *The International Journal of Robotics Research*, vol. 33, no. 5, pp. 736–752, 2014.

[9] R. Deimel and O. Brock, "A novel type of compliant and underactuated robotic hand for dexterous grasping," *The International Journal of Robotics Research*, vol. 35, no. 1-3, pp. 161–185, 2016.

[10] J. Zhou, J. Yi, X. Chen, Z. Liu, and Z. Wang, "Bcl-13: A 13-dof soft robotic hand for dexterous grasping and in-hand manipulation," *IEEE Robotics and Automation Letters*, vol. 3, no. 4, pp. 3379–3386, 2018.

[11] J. Zhou, X. Chen, U. Chang, J.-T. Lu, C. C. Y. Leung, Y. Chen, Y. Hu, and Z. Wang, "A soft-robotic approach to anthropomorphic robotic hand dexterity," *IEEE Access*, vol. 7, p. 101483–101495, 2019.

[12] K. C. Galloway, K. P. Becker, B. Phillips, J. Kirby, S. Licht, D. Tchernov, R. J. Wood, and D. F. Gruber, "Soft Robotic Grippers for Biological Sampling on Deep Reefs," *Soft Robotics*, vol. 3, no. 1, p. soro.2015.0019, 2016.

[13] N. R. Sinatra, C. B. Teeple, D. M. Vogt, K. K. Parker, D. F. Gruber, and R. J. Wood, "Ultragentle manipulation of delicate structures using a soft robotic gripper," *Science Robotics*, vol. 4, no. 33, 2019.

[14] B. Shih, D. Drotman, C. Christianson, Z. Huo, R. White, H. I. Christensen, and M. T. Tolley, "Custom soft robotic gripper sensor skins for haptic object visualization," in *2017 IEEE/RSJ International Conference on Intelligent Robots and Systems (IROS)*. IEEE, Sep 2017, p. 494–501.

[15] B. Sundaralingam and T. Hermans, "Geometric in-hand regrasp planning: Alternating optimization of finger gaits and in-grasp manipulation," in *2018 IEEE International Conference on Robotics and Automation (ICRA)*, May 2018, pp. 231–238.

[16] Y. Fan, W. Gao, W. Chen, and M. Tomizuka, "Real-time finger gaits planning for dexterous manipulation," *IFAC-PapersOnLine*, vol. 50, no. 1, p. 12765–12772, Jul 2017.

[17] L. Han and J. Trinkle, "Dextrous manipulation by rolling and finger gaiting," in *Proceedings. 1998 IEEE International Conference on Robotics and Automation (Cat. No.98CH36146)*, vol. 1. IEEE, 1998, p. 730–735.

[18] O. M. Andrychowicz, B. Baker, M. Chociej, R. Józefowicz, B. McGrew, J. Pachocki, A. Petron, M. Plappert, G. Powell, A. Ray, and et al., "Learning dexterous in-hand manipulation," *The International Journal of Robotics Research*, vol. 39, no. 1, p. 3–20, Jan 2020.

[19] Soft Robotics Inc., "5 reasons to automate your bakery operations," *White Paper*, 2019. [Online]. Available: http://info.softroboticsinc.com/automate-bakery-with-robotics

[20] W. Friedl, H. Höppner, F. Schmidt, M. A. Roa, and M. Grebenstein, "Clash: Compliant low cost antagonistic servo hands," in *2018 IEEE/RSJ International Conference on Intelligent Robots and Systems (IROS)*. IEEE, 2018, pp. 6469–6476.

[21] R. R. Ma and A. M. Dollar, "An underactuated hand for efficient finger-gaiting-based dexterous manipulation," in *2014 IEEE International Conference on Robotics and Biomimetics (ROBIO 2014)*. IEEE, Dec 2014, p. 2214–2219.

[22] M. Higashimori, H. Jeong, I. Ishii, M. Kaneko, A. Namiki, and M. Ishikawa, "A new four-fingered robot hand with dual turning mechanism," in *Proceedings of the 2005 IEEE International Conference on Robotics and Automation*. IEEE, 2005, p. 2679–2684.

[23] B. Calli, A. Walsman, A. Singh, S. Srinivasa, P. Abbeel, and A. M. Dollar, "Benchmarking in manipulation research: Using the yale-cmu-berkeley object and model set," *IEEE Robotics & Automation Magazine*, vol. 22, no. 3, pp. 36–52, 2015.

[24] C. B. Teeple, T. N. Koutros, M. A. Graule, and R. J. Wood, "Multi-segment soft robotic fingers enable robust precision grasping," *International Journal of Robotics Research*, 2020.

[25] B. W. McInroe, C. L. Chen, K. Y. Goldberg, R. Bajcsy, and R. S. Fearing, "Towards a soft fingertip with integrated sensing and actuation," in *2018 IEEE/RSJ International Conference on Intelligent Robots and Systems (IROS)*, Oct 2018, pp. 6437–6444.

[26] M. R. Cutkosky and P. K. Wright, "Friction, Stability and the Design of Robotic Fingers," *The International Journal of Robotics Research*, vol. 5, no. 4, pp. 20–37, 1986.

[27] C. B. Teeple, "Ctrl-p, v2.0," *Computer Software*, Feb. 2020. [Online]. Available: https://github.com/cbteeple/pressure_controller

[28] Tracker, "Tracker video analysis and modeling software, version 5.0.7," *Computer Software*, Mar 2019. [Online]. Available: https://physlets.org/tracker

[29] P. Paoletti, G. W. Jones, and L. Mahadevan, "Grasping with a soft glove: intrinsic impedance control in pneumatic actuators," *Journal of The Royal Society Interface*, vol. 14, no. 128, p. 20160867, Mar 2017.